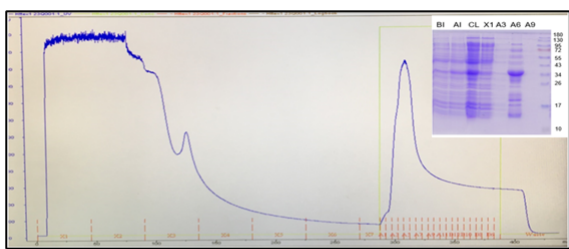
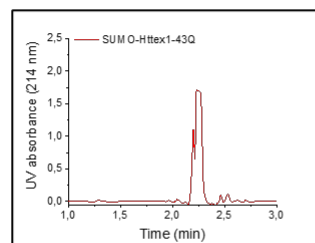
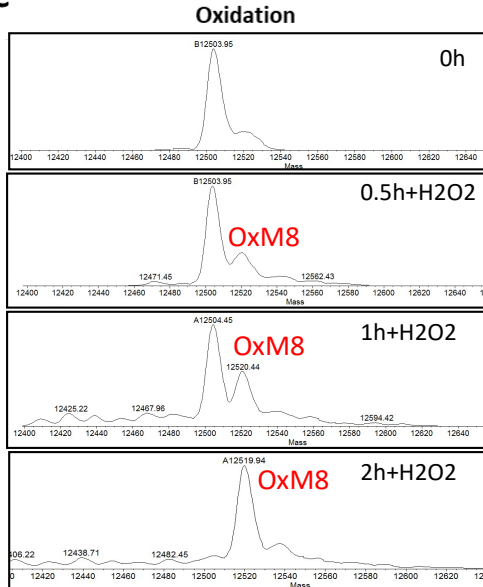
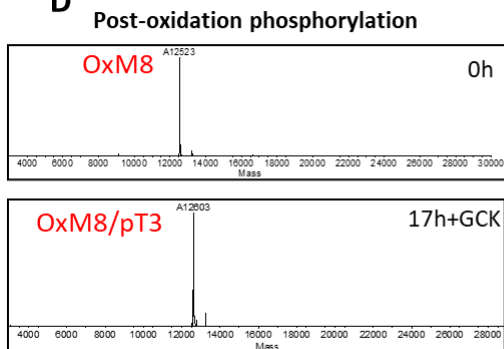
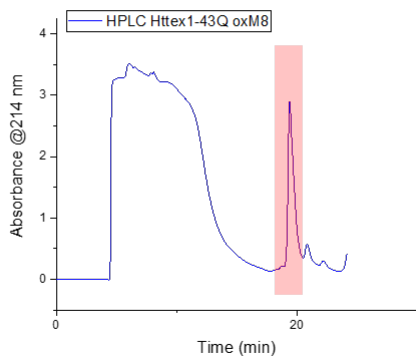
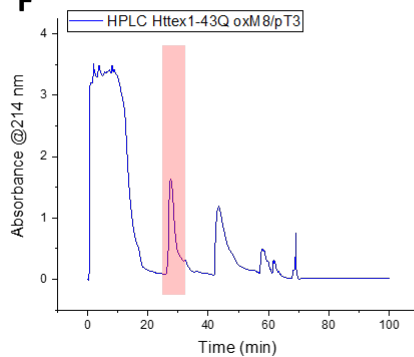
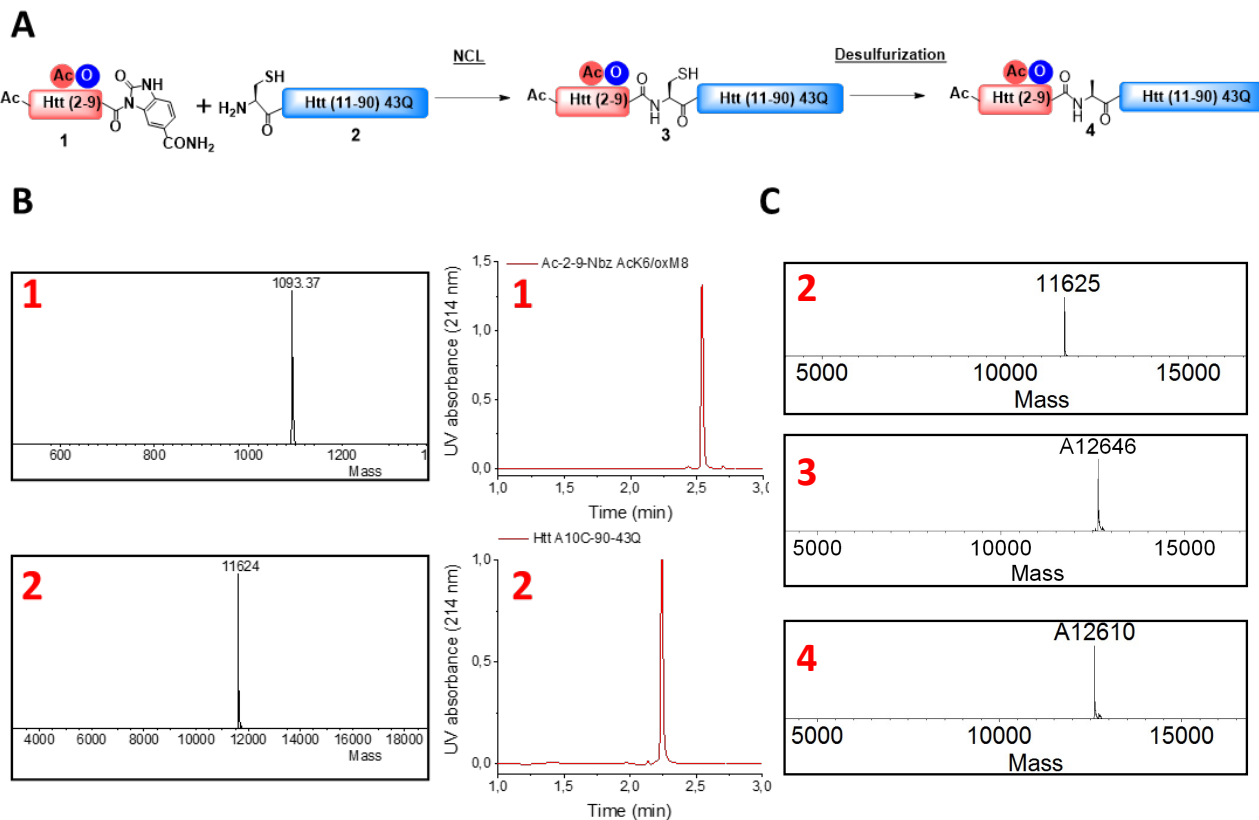




*Supplementary Material*

**A****B****C****D****E****F**

**Figure S1.** **(A)** Representative chromatogram of the IMAC purification of SUMO-mHttex1 and the analysis by SDS-PAGE of the purification fractions. **(B)** Analysis by UPLC of the fusion SUMO-mHttex1 after IMAC purifications. **(C)** Monitoring by ESI/MS of SUMO-mHttex1 oxidation by H<sub>2</sub>O<sub>2</sub> overtime after an analytical SUMO tag cleavage by ULP1. **(D)** Monitoring of SUMO-mHttex1 phosphorylation by GCK after an analytical SUMO tag cleavage by ULP1. **(E-F)** RP-HPLC chromatograms for the purification of mHttex1 oxM8 (E) and mHttex1 oxM8/pT3 (F). (protein of interest is highlighted in red).



**Figure S2.** (A) Schematic representation for the semisynthetic strategy used for the generation of mHttex1-oxM8/AcK6 (**4**) (adapted from [30]). (B) Characterization by ESI/MS and UPLC of Htt Ac-2-9-Nbz oxM8/AcK6 (**1**) and Htt A10C-90 43Q (**2**), both are the starting material for the semi-synthesis. The native chemical ligation of (**1**) and (**2**) was performed in (8 M urea, 0.5 M L-Proline, 30 mM D-Trehalose, 100 mM TCEP, pH 7), and the ligation was monitored by ESI/MS (C). When the NCL was completed, the reaction solution containing Httex1-43Q-oxM8/AcK6 A10C (**3**) was dialyzed and lyophilized and then desulfurized in 100 mM TCEP, 40 mM L-methionine, 20 vol% acetic acid in H<sub>2</sub>O pH 1, the desulfurization of Cys to Ala was monitored by ESI/MS.

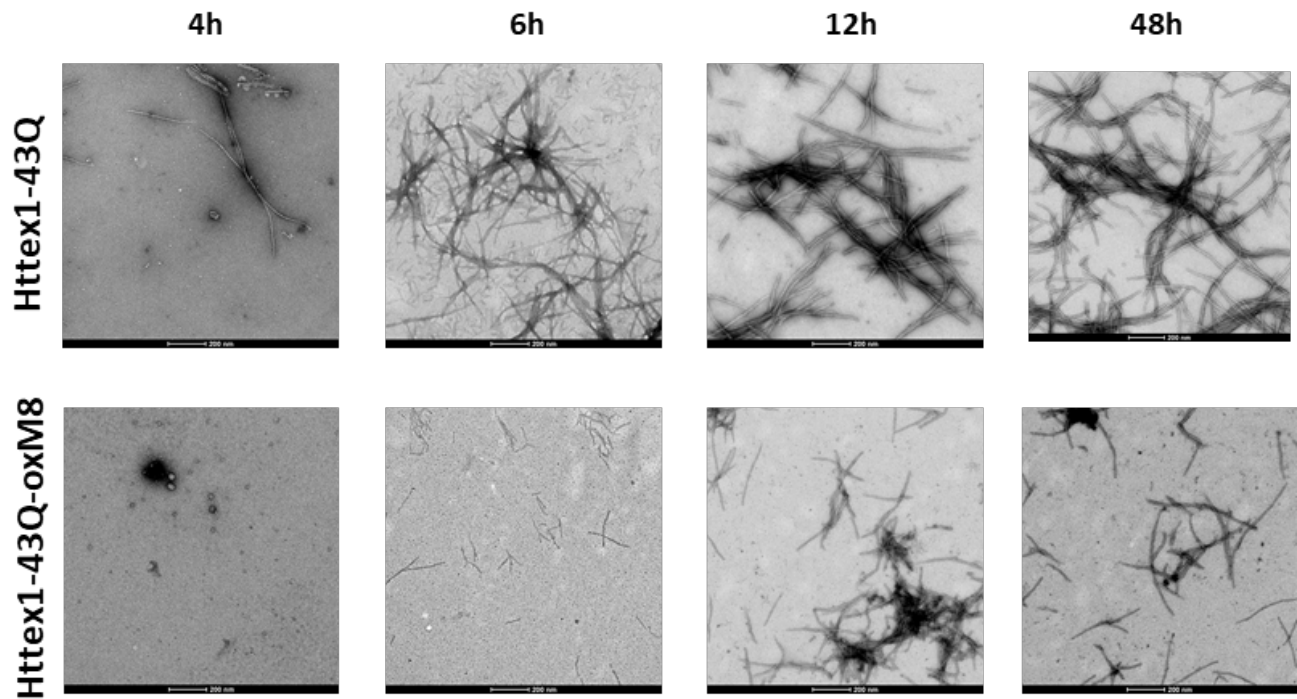


**Figure S3.** Over-time aggregation monitoring by electron microscopy of Httex1-43Q-oxM8 compared to unmodified Httex1-43Q (at 10  $\mu\text{M}$ ).

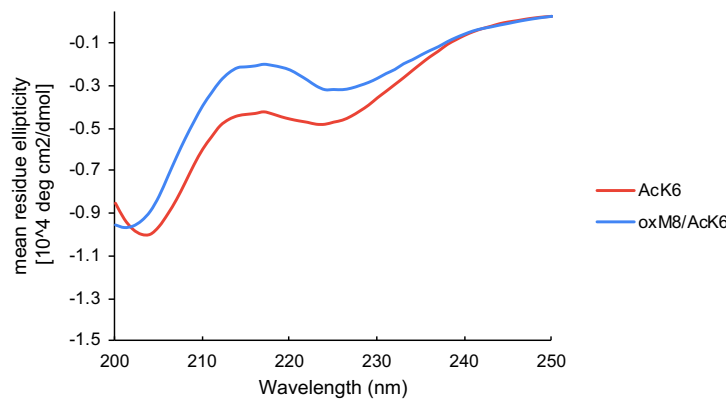
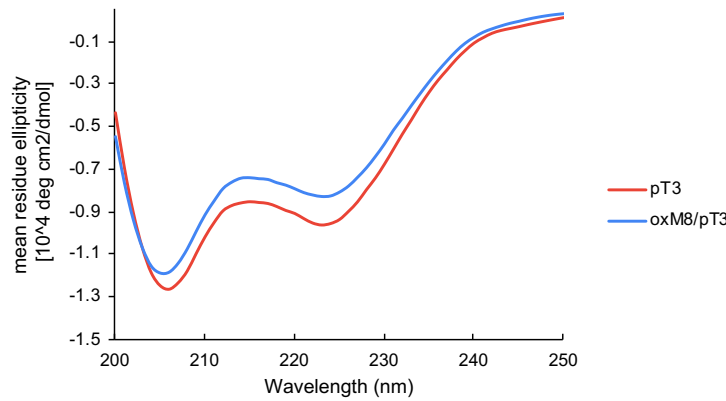
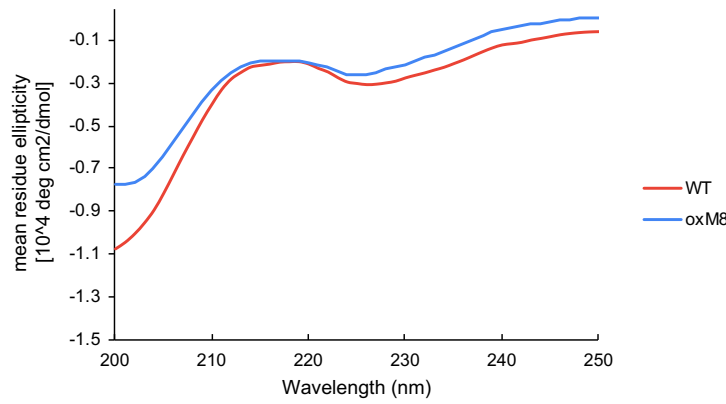


**Figure S4.** Far-UV CD spectra of Nt17-WT, and Nt17-oxM8, Nt17-AcK6, Nt17-AcK6/oxM8, Nt17-pT3 and Nt17-pT3/oxM8 at 60  $\mu$ M.

**Table S1:** Helical content (%) calculated from 3 repeats for the different peptides at 60  $\mu$ M.

Nt17 peptide	CD Helical content (%)
WT	0.1 $\pm$ 0.1
oxM8	1.7 $\pm$ 0.5
pT3	21.8 $\pm$ 0.7
pT3/oxM8	18.9 $\pm$ 0.5
AcK6	5.0 $\pm$ 0.2
AcK6/oxM8	1.6 $\pm$ 0.2

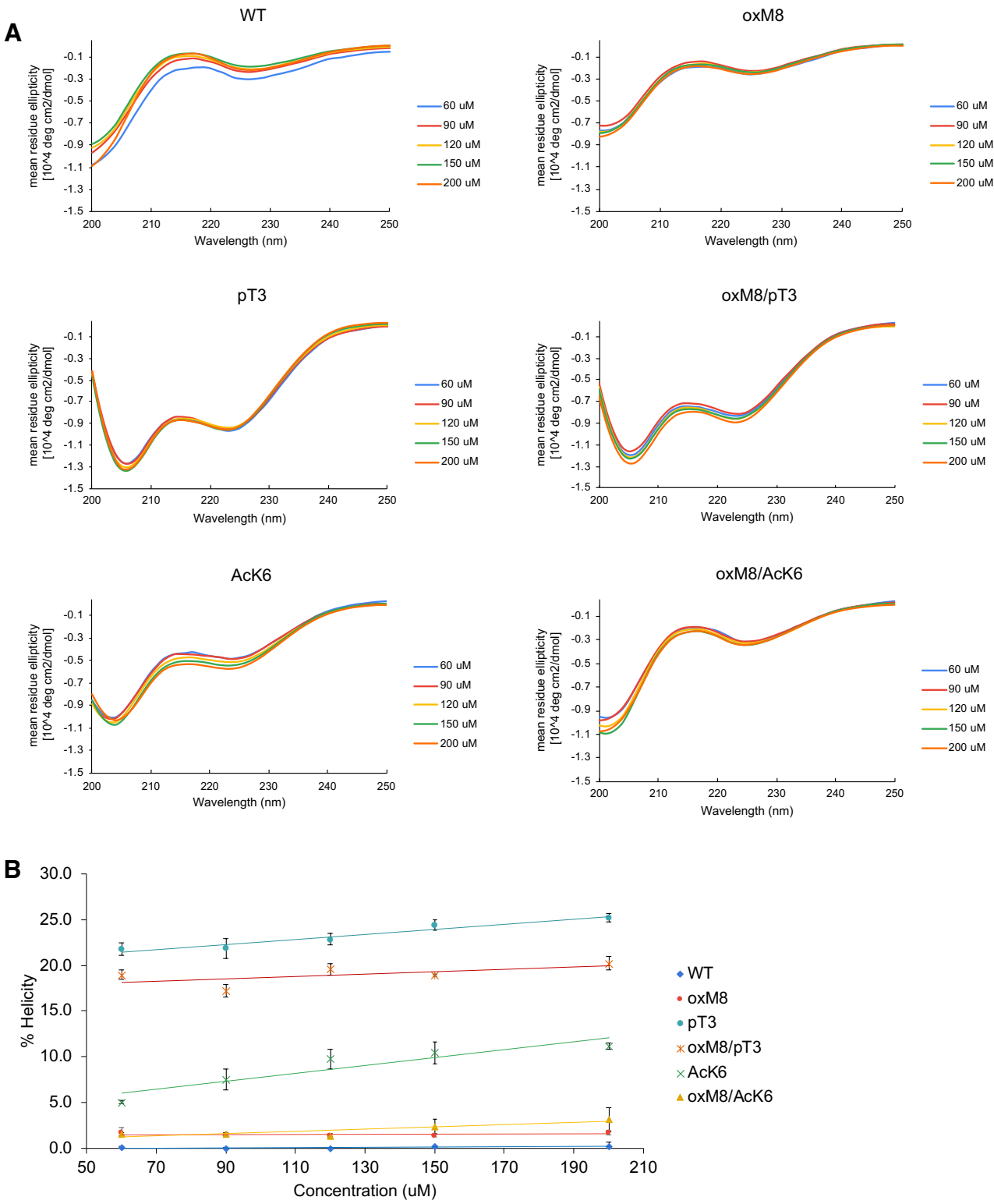


**Figure S5. (A)** Far-UV CD spectra of Nt17-WT, and Nt17-oxM8, Nt17-AcK6, Nt17-AcK6/oxM8, Nt17-pT3 and Nt17-pT3/oxM8 at 60, 90, 120, 150, and 200  $\mu$ M. **(B)** Helical content for the peptides in the function of the different concentrations. The error bars indicate the standard deviations calculated from 3 repeats.

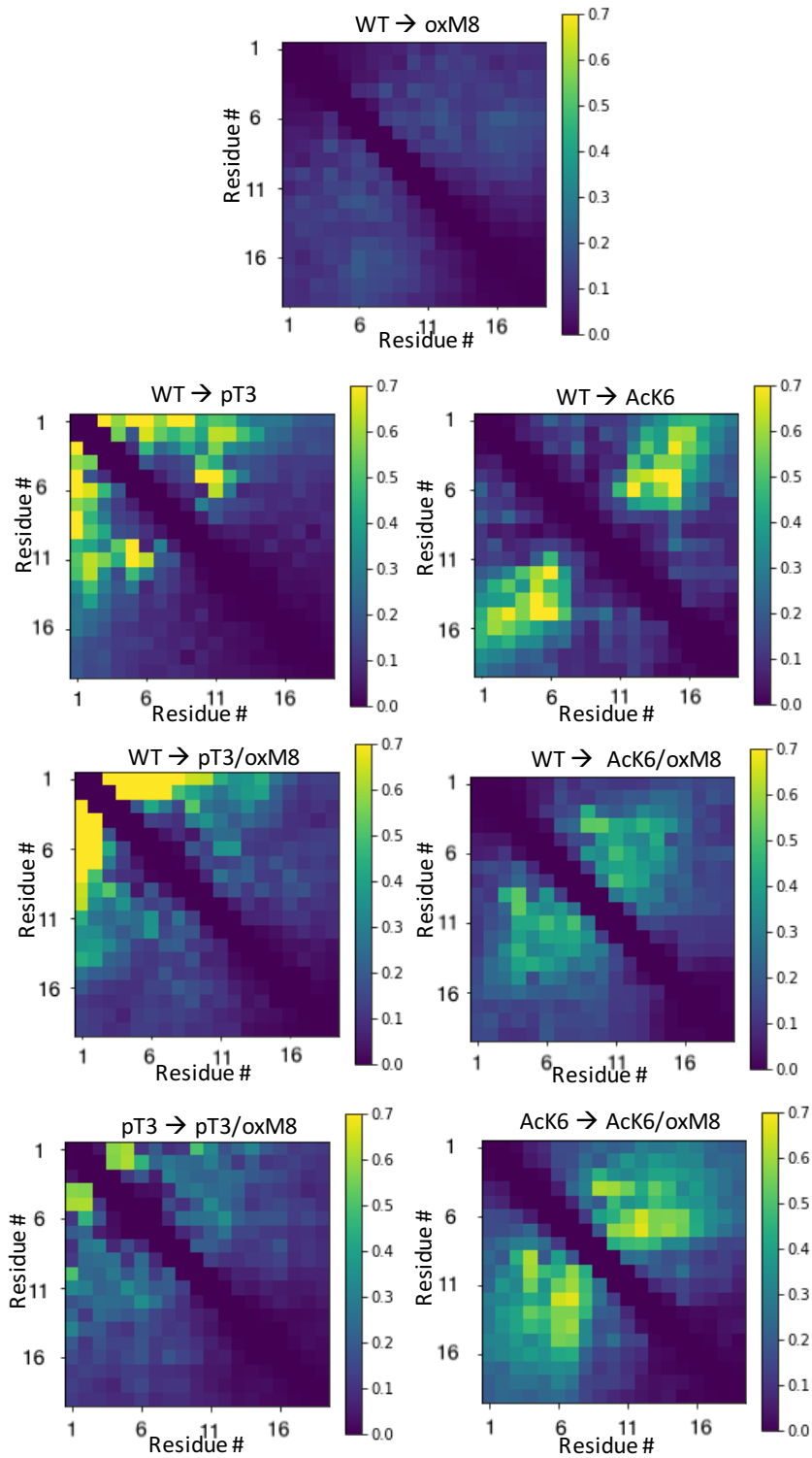


**Figure S6. The Kullback–Leibler divergence of pairwise distances of  $\text{C}\alpha$ .** For each MD of Nt19, the distances between all pairs of  $\text{C}\alpha$  in Nt19 were calculated. The differences in residue-residue contact were quantified using the Kullback-Leibler divergence from its reference histogram of distances.